Available online at www.sciencedirect.com
SCIENCE DIRECT®
Pergamon
Acta Materialia 51 (2003) 4059–4071
Acta MATERIALIA
www.actamat-journals.com

Crossover from grain boundary sliding to rotational deformation in nanocrystalline materials

M. Yu. Gutkin *, I.A. Ovid'ko, N.V. Skiba

Institute of Problems of Mechanical Engineering, Russian Academy of Sciences, Bolshoj 61, Vasil. Ostrov, St Petersburg 199178, Russia

Received 7 March 2003; received in revised form 16 April 2003; accepted 21 April 2003

Abstract

A theoretical model is suggested which describes cooperative action of grain boundary (GB) sliding and rotational deformation in mechanically loaded nanocrystalline materials. Focuses are placed on the crossover from GB sliding to rotational deformation occurring at triple junctions of GBs. In the framework of the model, gliding GB dislocations at triple junctions of GBs split into dislocations that climb along the adjacent boundaries. The splitting processes repeatedly occurring at triple junctions give rise to climb of GB dislocation walls that carry rotational deformation accompanied by crystal lattice rotation in grains of nanocrystalline materials. The role of GB sliding, rotational deformation and conventional dislocation slip in high-strain-rate superplastic flow in nanocrystalline materials is discussed.

Keywords: Deformation; Grain boundaries; Dislocations; Nanostructures

1. Introduction

Nanocrystalline materials exhibit outstanding mechanical properties opening a range of new applications in high technologies [1–3]. The unique deformation behavior of nanocrystalline materials is treated to be caused by suppression of conventional lattice dislocation slip (which dominates in coarse-grained materials) and effective action of alternative deformation mechanisms occurring through motion of grain boundary (GB) defects (see [4–12]). These mechanisms are GB sliding [4–7], GB diffusional creep [8–10] and triple junction diffusional creep [11] (for a review, see [12]). Recently, rotational deformation mode occurring through motion of GB disclination dipoles has been considered as the deformation mechanism effectively contributing to plastic flow in nanocrystalline materials [13–16]. The idea on rotational deformation is confirmed by experimental observations of disclination dipoles and grain rotations in mechanically loaded nanocrystalline materials [13,17].

Theoretical models [14–16] of rotational deformation mode in nanocrystalline materials commonly deal with the only movement of GB disclination dipoles along parallel GB facets,

* Corresponding author. Tel.: +7-812-3214764; fax: +7-812-3214771.
E-mail addresses: gutkin@def.ipme.ru (M.Yu. Gutkin); ovidko@def.ipme.ru (I.A. Ovid'ko).

1359-6454/03/$30.00
doi:10.1016/S1359-6454(03)00226-X

accompanied by crystal lattice rotation between these facets. In coarse-grained materials, the disclination dipoles are also supposed to move along parallel planes, thus forming the so-called misorientation bands [18–20]. However, this view is oversimplified in the case of nanocrystalline materials where GBs are short, curved and form triple junctions whose volume fraction is extremely high. Also, theoretical models of the rotational deformation mechanism and other deformation mechanisms operating in nanocrystalline solids, describe these mechanisms at the atomic level in terms of defects of atomic structures, with subsequent extrapolation to a description of their contributions to the macroscopic deformation behavior of a nanocrystalline specimen as a whole. In doing so, it is commonly assumed that either one mechanism is dominant or several mechanisms simultaneously contribute to plastic flow which act independently from each other. In the former case, if GB sliding dominates, accommodation mechanisms (like local GB migration [4,5]) are considered. In the second case, a grain size distribution in a nanocrystalline specimen is taken into account in calculation of the yield stress as the averaged (over grain sizes) value with different deformation mechanisms independently acting in grains with sizes being in different ranges [8,9,11]. However, nanocrystalline materials are aggregates of nanosized grains in which different deformation mechanisms, in general, strongly influence each other. That is, there is a kind of effective interaction between deformation modes in nanocrystalline materials, which definitely should be taken into consideration. In particular, it is of crucial importance in high-strain-rate superplasticity of nanocrystalline materials, which, according to experimental data [1,17,21–23], involves GB sliding, grain rotations and lattice dislocation slip as the key deformation modes strongly influence each other.

The main aim of this paper is to elaborate a theoretical model describing the combined action of GB sliding and rotational deformation mode in nanocrystalline materials, with focuses placed on the crossover from GB sliding to rotation deformation occurring at triple junctions of GBs. With results of the model, the role of the combined action of these deformation mechanisms and lattice dislocation slip in high-strain-rate superplastic deformation of nanocrystalline materials is discussed.

2. Splitting of gliding grain boundary dislocations at triple junction into climbing dislocations (small-scale view)

GB sliding which is treated to be the dominant mode of superplasticity in nano- and microcrystalline materials occurs via motion of gliding GB dislocations. They have Burgers vectors that are parallel with corresponding GB planes along which these dislocations glide. Triple junctions of GBs, where GB planes change their orientations, serve as obstacles for the GB dislocation motion. In these circumstances, splitting of gliding GB dislocations can occur at triple junctions, resulting in the formation of sessile dislocations and gliding dislocations providing the further GB sliding along the adjacent GBs [7]. However, in general, GB dislocations stopped at a triple junction are also capable of being split into climbing GB dislocations (Fig. 1). When this process repeatedly occurs at a triple junction, it results in the formation of two walls of dislocations climbing along the GBs adjacent to the triple junction (Fig. 1). The climbing dislocation walls cause the rotational deformation, in which case the repeatedly occurring splitting of gliding GB dislocations at the triple junction provides the crossover from the GB sliding to the rotational deformation mode.

Thus, the crossover occurs through the splitting of a pile-up of gliding GB dislocations into climbing dislocation walls that provide crystal lattice rotation in a nanograin as a whole. In doing so, the crossover is sensitive to small- and large-scale transformations of the defect structure which occur in the vicinity of the triple junction and the nanograin as a whole, respectively. In this context, we will theoretically examine the defect structure transformations at both the small- and large-scale levels. First, we will consider at a small-scale level, in terms of GB dislocations, an elementary act of the crossover from the GB sliding to the rotational deformation. The act is the splitting of a gliding

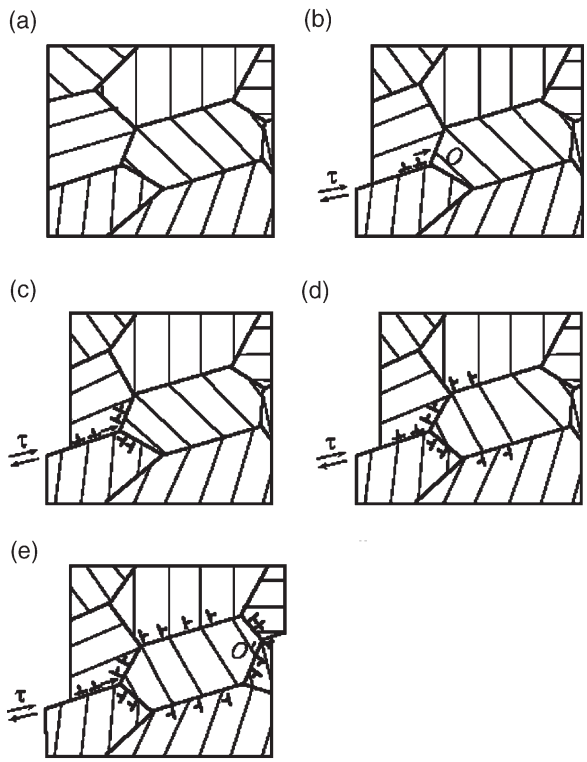

Fig. 1. Combined action of GB sliding and rotational deformation mode. (a) Nanocrystalline specimen in a non-deformed state. (b) GB sliding occurs via motion of gliding GB dislocations under shear stress action. (c) Gliding dislocations split at triple junction O of GBs into climbing dislocations. (d) The splitting of gliding GB dislocations repeatedly occurs causing the formation of walls of GB dislocations whose climb is accompanied by crystal lattice rotation in a grain. (e) Climbing dislocations reach triple junction O' where they converge into gliding dislocations causing further GB sliding.

GB dislocation into two climbing GB dislocations at a triple junction; for details, see the rest of this section. Then, we will consider the crossover from the GB sliding to the rotational deformation at a large-scale level in terms of GB dislocation groups involved in the crossover. More precisely, in the framework of large-scale analysis (Section 3), we will consider disclinations serving as models of ragged walls of climbing GB dislocations, and superdislocations serving as models of the pile-ups of GB dislocations stopped at triple junctions.

In the rest of this section, we will theoretically examine the crossover from the GB sliding to the rotational deformation at a small-scale level. Let us consider a two-dimensional model of GB dislocation configurations whose transformations represent elementary acts of the crossover in question. Such an elementary act is the splitting of a head GB dislocation at a triple junction into two GB dislocations which climb along the GBs adjacent to the triple junction. Let us analyze the energy characteristics of the splitting which occurs under the action of a shear stress τ. The splitting of the head GB dislocation of the pile-up into the two climbing GB dislocations (Fig. 2) is characterized by the difference $\Delta W = W_2 - W_1$ between the energies of the final (W_2) and initial (W_1) states of the defect configuration under consideration. The splitting is energetically favorable (unfavorable), if $\Delta W < 0$ ($\Delta W > 0$, respectively). The equation $\Delta W = 0$ gives a set of critical values of parameters for the defect configuration, at which the splitting becomes energetically favorable.

In calculating the energy characteristics of the splitting, for definiteness and simplicity, we make the following model assumptions: (i) Magnitudes of the Burgers vectors of all GB dislocations belonging to the dislocation pile-up are the same. (ii) The plane of the shear stress τ action is parallel with the plane of the GB where the pile-up is located. (iii) After the splitting of the head dislo-

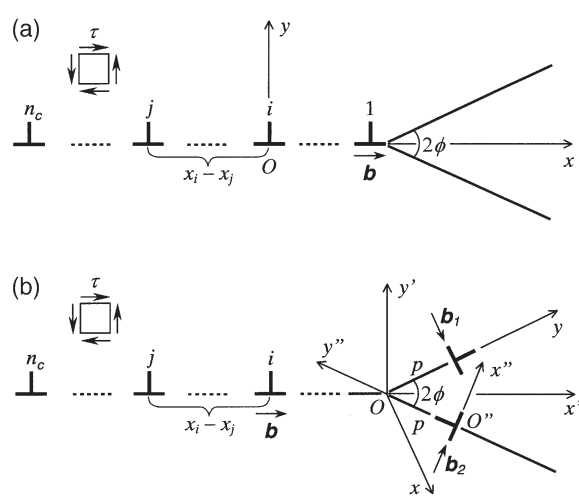

Fig. 2. Splitting of the (a) head dislocation of a GB dislocation pile-up at a triple junction into (b) two dislocations that climb along the adjacent GBs. Coordinate systems Oxy, $Ox'y'$ and $O''x''y''$ are shown which are used in calculations (see text).

cation of the pile-up, the residual GB dislocations composing the pile-up do not move from their initial positions. These assumptions do not influence essentially the quantitative results of our consideration and, at the same time, allow us to find analytical expressions for the energy characteristics of defects involved in the splitting.

The initial defect configuration represents a pile-up of n_c gliding GB dislocations near a triple junction (Fig. 2(a)). Its energy W_1 consists of two terms

$$W_1 = E_1^{\text{pile-up}} + E_\Sigma^{\text{b–b}}, \tag{1}$$

where $E_1^{\text{pile-up}}$ is the sum of the proper energies of GB dislocations composing the pile-up, and $E_\Sigma^{\text{b–b}}$ is the energy that characterizes pair interactions between all these dislocations.

We will describe the first term in Eq. (1), $E_1^{\text{pile-up}}$, a bit later, while describing the corresponding term of the energy W_2.

In order to find the energy $E_\Sigma^{\text{b–b}}$, let us calculate the energy $E_{ij}^{\text{b–b}}$ that characterizes elastic interaction between the ith and jth GB dislocations belonging to the pile-up. The energy that characterizes elastic interaction between two defects can be calculated as the work spent to transfer one defect from a free surface of a solid to its current position in the stress field created by another defect [24]. Therefore the energy $E_{ij}^{\text{b–b}}$ can be calculated using the formula

$$E_{ij}^{\text{b–b}} = -b\int_{-R}^{-(x_j-x_i)} \sigma_{xy}^i(x,y=0)\,dx, \tag{2}$$

where x_i and x_j are the positions of GB dislocations within the pile-up (they are calculated as the roots of the first derivative of the Laguerre polynomial [25]), σ_{xy}^i is the ith dislocation-induced shear stress acting on the jth dislocation. This stress is written in coordinate system Oxy (Fig. 2 (a)) as follows

$$\sigma_{xy}^i = Dbx\frac{x^2-y^2}{(x^2+y^2)^2}, \tag{3}$$

where $D = G/2\pi(1-\nu)$. With Eq. (3) substituted to formula (2), we have

$$E_{ij}^{\text{b–b}} = Db^2\ln\frac{R}{x_i-x_j}, \tag{4}$$

where R denotes the screening length of the dislocation stress field.

The energy $E_\Sigma^{\text{b–b}}$ that characterizes pair interactions between all GB dislocations belonging to the pile-up (Fig. 2(a)) is the sum of energies E_{ij} over the GB dislocation indices i and j ($i \neq j$)

$$E_\Sigma^{\text{b–b}} = \sum_{i=1}^{n_c-1}\sum_{j=i+1}^{n_c} E_{ij}^{\text{b–b}} = Db^2\sum_{i=1}^{n_c-1}\sum_{j=i+1}^{n_c}\ln\frac{R}{x_i-x_j}. \tag{5}$$

The energy of the defect configuration (Fig. 2(b)) resulted from the splitting of the head dislocation belonging to the GB dislocation pile-up consists of seven terms

$$W_2 = E_2^{\text{pile-up}} + 2E_{\text{disl}}^{\text{self}} + E'^{\text{b–b}}_\Sigma + E_{\Sigma^1}^{\text{b}_1\text{–b}} + E_{\Sigma^2}^{\text{b}_2\text{–b}} + E^{\text{b}_1\text{–b}_2} + 2E_\tau. \tag{6}$$

Here $E_2^{\text{pile-up}}$ denotes the sum of proper energies of the GB dislocations belonging to the pile-up after the splitting, $2E_{\text{disl}}^{\text{self}}$ the sum of proper energies of the two GB dislocations resulted from the splitting of the head dislocation, $E'^{\text{b–b}}_\Sigma$ the energy of pair interactions between all GB dislocations composing the pile-up, $E_{\Sigma^1}^{\text{b}_1\text{–b}}$ ($E_{\Sigma^2}^{\text{b}_2\text{–b}}$, respectively) the energy that characterizes interaction between GB dislocations of the pile-up and the GB dislocation resulted from the slitting and characterized by Burgers vector $\boldsymbol{b}_1$ ($\boldsymbol{b}_2$, respectively), $E^{\text{b}_1\text{–b}_2}$ the energy of interaction between the two dislocations formed due to the splitting, and E_τ the effective work of the shear stress τ, spent to transfer these two GB dislocations along the GBs adjacent to the triple junction.

The pile-up after the splitting of its head dislocation (Fig. 2(b)) contains n_c-1 GB dislocations. To simplify our calculations of the energy characteristics of these dislocations, we assume that their positions remain unchanged during the splitting of the head dislocation. This assumption is reasonable in at least the situation where the GB dislocations resulted from the splitting are close to the triple junction (Fig. 2(b)). In the situation discussed, the energy $E'^{\text{b–b}}_\Sigma$ that characterizes interaction between all GB dislocations composing the pile-up represents the sum of the energies $E_{ij}^{\text{b–b}}$ over indices of n_c-1 dislocations. That is

$$E'^{\mathrm{b}-\mathrm{b}}_{\Sigma} = \sum_{i=2}^{n_c-1}\sum_{j=i+1}^{n_c} E^{\mathrm{b}-\mathrm{b}}_{ij} = Db^2\sum_{i=2}^{n_c-1}\sum_{j=i+1}^{n_c}\ln\frac{R}{x_i-x_j}. \tag{7}$$

The energy $E^{\mathrm{b}-\mathrm{b}_1}_{\Sigma}$ figuring on the r.h.s. of formula (6) is the sum of energies $E^{\mathrm{b}-\mathrm{b}_1}_i$ characterizing interaction between the ith GB dislocation of the pile-up and the resultant dislocation with the Burgers vector $\boldsymbol{b}_1$ which, for brevity, hereinafter will be denoted as $\boldsymbol{b}_1$-dislocation. The energy $E^{\mathrm{b}_1-\mathrm{b}}_i$ can be calculated as the work spent to the generation of the ith dislocation in the shear stress τ_{b_1} created by the $\boldsymbol{b}_1$-dislocation [24]. The $\boldsymbol{b}_1$-dislocation distant by p from the triple junction O creates the stress field having the following components in the Oxy coordinate system (Fig. 2(b)) [26]

$$\sigma^{\mathrm{b}_1}_{xx} = -Db_1(y-p)\frac{3x^2+(y-p)^2}{[x^2+(y-p)^2]^2},$$
$$\sigma^{\mathrm{b}_1}_{yy} = Db_1(y-p)\frac{x^2-(y-p)^2}{[x^2+(y-p)^2]^2}, \tag{8}$$
$$\sigma^{\mathrm{b}_1}_{xy} = Db_1x\frac{x^2-(y-p)^2}{[x^2+(y-p)^2]^2}.$$

Let us introduce a new coordinate system $Ox'y'$ (Fig. 2(b)) in which the shear stress τ_{b_1} acting in the plane $y'=0$, is expressed through the stress field components (8) as follows

$$\tau_{\mathrm{b}_1} = \sigma^{\mathrm{b}_1}_{xx}\alpha_1\alpha_2 + \sigma^{\mathrm{b}_1}_{yy}\beta_1\beta_2 + \sigma^{\mathrm{b}_1}_{zz}\gamma_1\gamma_2 + \sigma^{\mathrm{b}_1}_{xy}(\alpha_1\beta_2+\alpha_2\beta_1) + \sigma^{\mathrm{b}_1}_{yz}(\beta_1\gamma_2+\beta_2\gamma_1) + \sigma^{\mathrm{b}_1}_{zx}(\gamma_1\alpha_2+\gamma_2\alpha_1), \tag{9}$$

where $\alpha_1=\cos(x',x)=\cos(\pi/2-\phi)=\sin\phi$, $\beta_1=\cos(x',y)=\cos\phi$, $\gamma_1=\cos(x',z)=0$, $\alpha_2=\cos(y',x)=\cos(\pi+\phi)=-\cos\phi$, $\beta_2=\cos(y',y)=\cos(\pi/2-\phi)=\sin\phi$, $\gamma_2=\cos(y',z)=0$. With these formulas substituted to (9), we get

$$\tau_{\mathrm{b}_1} = \frac{1}{2}(\sigma^{\mathrm{b}_1}_{yy}-\sigma^{\mathrm{b}_1}_{xx})\sin 2\phi - \sigma^{\mathrm{b}_1}_{xy}\cos 2\phi. \tag{10}$$

Using the following relationships (written with account for $y'=0$)

$$x = x'\cos\left(\frac{\pi}{2}-\phi\right) = x'\sin\phi;$$
$$y = x'\sin\left(\frac{\pi}{2}-\phi\right) = x'\cos\phi, \tag{11}$$

Eq. (10) can be rewritten through x' as follows

$$\tau_{\mathrm{b}_1} = Db_1\frac{x'(x'^2-2x'p\cos\phi+p^2\cos 2\phi)\sin\phi}{(x'^2-2x'p\cos\phi+p^2)^2}. \tag{12}$$

The energy $E^{\mathrm{b}_1-\mathrm{b}}_i$ that characterizes interaction between the ith dislocation of the pile-up and the $\boldsymbol{b}_1$-dislocation is given by the following general formula

$$E^{\mathrm{b}_1-\mathrm{b}}_i = -b\int_{-R}^{-x_i}\tau_{\mathrm{b}_1}(x',y'=0)\,\mathrm{d}x', \tag{13}$$

where x_i denotes the coordinate (along x'-axis) of the ith dislocation. With Eq. (12) substituted to formula (13), after integration, we have

$$E^{\mathrm{b}_1-\mathrm{b}}_i = Db_1b\left(\frac{(p^2+Rp\cos\phi)\sin\phi}{R^2+2Rp\cos\phi+p^2} - \frac{(p^2+x_ip\cos\phi)\sin\phi}{x_i^2+2x_ip\cos\phi+p^2} + \frac{1}{2}\sin\phi\ln\frac{R^2+2Rp\cos\phi+p^2}{x_i^2+2x_ip\cos\phi+p^2}\right). \tag{14}$$

The energy $E^{\mathrm{b}_1-\mathrm{b}}_{\Sigma}$ that characterizes interaction of the $\boldsymbol{b}_1$-dislocation with all GB dislocations composing the pile-up is calculated as the sum of energies $E^{\mathrm{b}_1-\mathrm{b}}_i$ given by formula (14). In the framework of our model, there is a mirror symmetry (with the plane $y'=0$ being the mirror plane) of the positions and Burgers vectors of the $\boldsymbol{b}_1$-dislocation and the resultant dislocation with Burgers vector $\boldsymbol{b}_2$, which, for brevity, hereinafter will be denoted as $\boldsymbol{b}_2$-dislocation. As a corollary, the energy $E^{\mathrm{b}_2-\mathrm{b}}_{\Sigma}$ that characterizes interaction between all GBs of the pile-up and the $\boldsymbol{b}_2$-dislocation is the same as $E^{\mathrm{b}_1-\mathrm{b}}_{\Sigma}$. Therefore, the total energy that characterizes interaction of the $\boldsymbol{b}_1$- and $\boldsymbol{b}_2$-dislocations with GB dislocations of the pile-up is given as

$$E^{\mathrm{b}_1-\mathrm{b}}_{\Sigma} + E^{\mathrm{b}_2-\mathrm{b}}_{\Sigma} = \sum_{i=1}^{n_c}(E^{\mathrm{b}_1-\mathrm{b}}_i + E^{\mathrm{b}_2-\mathrm{b}}_i). \tag{15}$$

Now let us calculate the energy $E^{b_1-b_2}$ that characterizes interaction between the $\boldsymbol{b}_1$- and $\boldsymbol{b}_2$-dislocations. The coordinate systems associated with these dislocations are presented in Fig. 2(b) which describes the situation where $\boldsymbol{b}_1$- and $\boldsymbol{b}_2$-dislocations are distant from the triple junction. In the coordinate system *Oxy*, the shear stress field which is created by the $\boldsymbol{b}_1$-dislocation and acts in the plane $y'' = 0$ (the gliding plane for the $\boldsymbol{b}_2$-dislocation) can be written through the stress field components in the following form

$$\tau_{b_1} = \sigma^{b_1}_{xx}\alpha_1\alpha_2 + \sigma^{b_1}_{yy}\beta_1\beta_2 + \sigma^{b_1}_{zz}\gamma_1\gamma_2 + \sigma^{b_1}_{xy}(\alpha_1\beta_2 + \alpha_2\beta_1) + \sigma^{b_1}_{yz}(\beta_1\gamma_2 + \beta_2\gamma_1) + \sigma^{b_1}_{zx}(\gamma_1\alpha_2 + \gamma_2\alpha_1), \quad (16)$$

where $\alpha_1 = \cos(x'',x) = \cos(\pi-2\phi) = -\cos 2\phi$, $\beta_1 = \cos(x'',y) = \cos(\pi/2-2\phi) = \sin 2\phi$, $\gamma_1 = \cos(x'',z) = 0$, $\alpha_2 = \cos(y'',x) = \cos(\pi/2 + 2\phi) = -\sin 2\phi$, $\beta_2 = \cos(y'',y) = \cos(\pi-2\phi) = -\cos 2\phi$, $\gamma_2 = \cos(y'',z) = 0$. With these cosines substituted to formula (16), we find

$$\tau_{b_1} = \frac{1}{2}(\sigma^{b_1}_{xx}-\sigma^{b_1}_{yy})\sin 4\phi + \sigma^{b_1}_{xy}\cos 4\phi. \quad (17)$$

Let us rewrite τ_{b_1} in coordinates x'' and y'' associated with the $\boldsymbol{b}_2$-dislocation and given by the following relationships (with account for $y'' = 0$)

$$x = -x''\cos 2\phi + p\sin 2\phi; \quad y = x''\sin 2\phi + p\cos 2\phi. \quad (18)$$

In doing so, we get

$$\tau_{b_1} = Db_1\frac{(p\sin 2\phi - x''\cos 2\phi)(x''^2 - 2x''p\sin 2\phi + 4p^2\cos 2\phi\sin^2\phi)}{(x''^2 - 2x''p\sin 2\phi + 4p^2\sin^2\phi)^2}. \quad (19)$$

Then the interaction energy $E^{b_1-b_2}$ is given by the general formula [24]

$$E^{b_1-b_2} = b_2\int_0^R \tau_{b_1}(x'',y''=0)\,dx''. \quad (20)$$

With Eq. (19) substituted to formula (20), integration gives

$$E^{b_1-b_2} = -\frac{Db_1b_2}{2}\left(\frac{2R^2}{R^2\,\mathrm{cosec}^2\,\phi - 4Rp\,\mathrm{ctg}\,\phi + 4p^2} + \cos 2\phi\ln\frac{R^2-2Rp\sin 2\phi + 4p^2\sin^2\phi}{4p^2\sin^2\phi}\right). \quad (21)$$

The sum of proper energies of GB dislocations composing the pile-up is [26]

$$E_1^{\text{pile-up}} = n_c\frac{Db^2}{2}\left(\ln\frac{R}{b} + 1\right) \quad (22)$$

before the splitting (Fig. 2(a)), and

$$E_2^{\text{pile-up}} = (n_c-1)\frac{Db^2}{2}\left(\ln\frac{R}{b} + 1\right) \quad (23)$$

after the splitting (Fig. 2(b)).

The $\boldsymbol{b}_1$- and $\boldsymbol{b}_2$-dislocations have the same proper energies

$$E^{b_i}_{\text{self}} = \frac{Db_i^2}{2}\left(\ln\frac{R}{b_i} + 1\right), \quad (24)$$

where $b_i = b/(2\sin\phi)$ ($i = 1,2$). The work spent to transfer the $\boldsymbol{b}_1$-dislocation by distance p under the shear stress τ is the same as that for the $\boldsymbol{b}_2$-dislocation and equal to

$$E_\tau = -b_1p\tau\sin 2\phi. \quad (25)$$

Thus, we have all terms figuring in the energy difference $\Delta W = W_2 - W_1$ that characterizes the splitting (Fig. 2) being an elementary act of the crossover from the GB sliding to the rotational deformation mode in nanocrystalline materials. The equation $\Delta W = 0$ gives a set of critical values of parameters of the defect configuration, at which the splitting becomes energetically favorable.

With formulas (1), (5)–(7), (14), (15), (21)–(25) for the energy characteristics, we have calculated the dependences of ΔW on the distance p moved by the two GB dislocations ($\boldsymbol{b}_1$- and $\boldsymbol{b}_2$- dislocations) resulted from the splitting, at various values of the angle 2ϕ that characterizes geometry of the triple junction. The following values for the system parameters have been used in calculations: $n_c = 5$, $R = 10^7b$ and $\tau = 0.005G$. These dependences presented in Fig. 3 show that the splitting—an

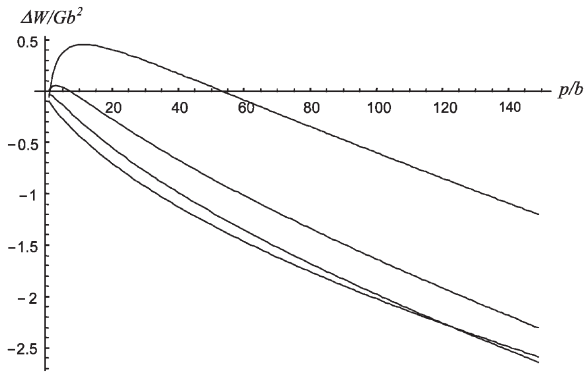

Fig. 3. Dependences of ΔW (in units of Gb^2) on distance p (in units of b) moved by climbing $\boldsymbol{b}_1$- and $\boldsymbol{b}_2$-dislocations, for $2\phi = 40$, 60, 80 and 120° (from top to bottom).

elementary act of the crossover from the GB sliding to the rotational mode—is energetically favorable at large values (80–100°) of the angle 2ϕ. In the study by Fedorov et al. [7] it has been demonstrated that the splitting of the head GB dislocation of a pile-up stopped at a triple junction into two, gliding and sessile, GB dislocations are energetically favorable at low values of the angle 2ϕ. That version of the splitting serves as an elementary act of the GB sliding at triple junctions [7]. Thus, the crossover from the GB sliding to the rotational deformation (Figs. 1 and 2) occurs effectively at triple junctions with large values of the angle 2ϕ, while the GB sliding itself occurs effectively at triple junctions with comparatively low values of the angle 2ϕ.

3. Cooperative action of grain boundary sliding and rotational deformation mode in nanocrystalline materials (large-scale view)

After the head GB dislocation has split into the $\boldsymbol{b}_1$- and $\boldsymbol{b}_2$-dislocations (Fig. 2(b)), their stress fields prevent movement of the second GB dislocation of the pile-up towards the triple junction where the splitting has occurred. When the climbing $\boldsymbol{b}_1$- and $\boldsymbol{b}_2$-dislocations move far from the triple junction, their effect on the second GB dislocation of the pile-up becomes weak. In this case the second dislocation of the pile-up moves to the triple junction where it splits into two GB dislocations climbing along the adjacent GBs. Such a splitting process repeatedly occurs transforming GB dislocations of the pile-up into the climbing GB dislocations (Fig. 1). These climbing dislocations form dislocation walls of finite extent at the two GBs adjacent to the triple junction.

Let us calculate the energy characteristics of the discussed evolution of the GB dislocation ensemble in the framework of a large-scale model. In doing so, the GB dislocation pile-up consisting of n_c dislocations in its initial state is represented as a superdislocation with the Burgers vector $\sigma_{xy}^{n_c b}$ (Fig. 4(a)). In order to describe a grain rotation accompanying the evolution of the GB dislocation ensemble, we assume that similar splitting processes occur at two opposite triple junctions of GBs surrounding a nano-sized grain. The GB dislocation pile-ups located near the opposite triple junctions consist of dislocations with the Burgers vectors of opposite signs, which tend to move

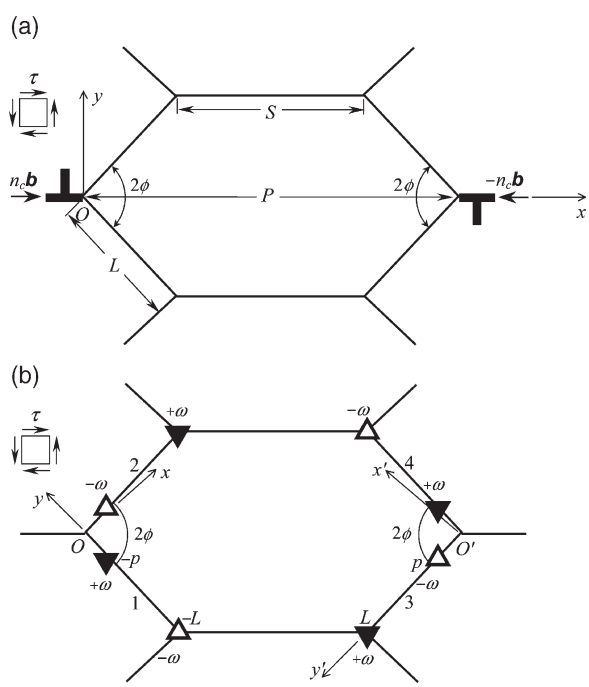

Fig. 4. Large-scale model of crossover from GB sliding to rotational deformation mode. (a) Two superdislocations (models of pile-ups of GB dislocations) are stopped at the opposite triple junctions. (b) Four disclination dipoles (models of climbing dislocation walls) are located at the GBs adjacent to the triple junctions.

under the shear stress action towards each other and are stopped by the triple junctions. Four GB dislocation walls of finite extent, following the general theory of disclinations in solids [18,19], are effectively represented as four dipoles of disclinations (Fig. 4(b)).

In calculating the energy characteristics of evolution of the GB dislocation ensemble, causing grain rotation, for definiteness and simplicity, we make the following model assumptions: (i) The grain is a hexagon with the angles 2ϕ characterizing the splitting processes at the opposite triple junctions being the same. (ii) Magnitudes of the Burgers vectors of all GB dislocations belonging to the dislocation pile-ups are the same. (iii) The plane of the shear stress τ action is parallel with planes of GBs where the GB dislocation pile-ups are located. (iv) All the disclinations modeling the walls of the climbing GB dislocations have the same strength magnitude ω.

The transformation of the GB dislocation ensemble (Fig. 4) is characterized by the difference $\Delta\tilde{W} = \tilde{W}_2 - \tilde{W}_1$ between the energies of the final ($\tilde{W}_2$) and initial ($\tilde{W}_1$) states of the ensemble. The transformation is energetically favorable (unfavorable), if $\Delta\tilde{W} < 0$ ($\Delta\tilde{W} > 0$, respectively). In the framework of the model discussed, the energy of the dislocation ensemble in its initial state (Fig. 4(a)) consists of the three terms

$$\tilde{W}_1 = 2E_1^{\text{pile-up}} + 2E_\Sigma^{\text{b–b}} + E_{\text{int}}^{n_c\text{b}-n_c\text{b}}, \tag{26}$$

where $E_1^{\text{pile-up}}$ denotes the sum of the proper energies of GB dislocations composing a pile-up, $E_\Sigma^{\text{b–b}}$ the energy that characterizes pair interactions between all GB dislocations composing one pile-up, and $E_{\text{int}}^{n_c\text{b}-n_c\text{b}}$ denotes the energy that characterizes pair interactions between GB dislocations belonging to the different pile-ups. $E_\Sigma^{\text{b–b}}$ and $E_1^{\text{pile-up}}$ have been calculated in Section 2 (see formulas (5) and (22), respectively).

Let us calculate $E_{\text{int}}^{n_c\text{b}-n_c\text{b}}$ in the approximation where the GB dislocation pile-ups are modeled as superdislocations (Fig. 4(a)). The shear stress $\sigma_{xy}^{n_c\text{b}}$ which is created by the superdislocation with the Burgers vector $n_c\boldsymbol{b}$ and acts on the superdislocation with the Burger vector $-n_c\boldsymbol{b}$ is as follows

$$\sigma_{xy}^{n_c\text{b}} = Dn_c b\frac{x(x^2-y^2)}{(x^2+y^2)^2}. \tag{27}$$

The energy of interaction between the two superdislocations then reads

$$E_{\text{int}}^{n_c\text{b}-n_c\text{b}} = -n_c b\int_P^R \sigma_{xy}^{n_c\text{b}}(x,y=0)\,\mathrm{d}x, \tag{28}$$

where P is the distance between the opposite triple junctions (Fig. 4(a)). With Eq. (27) substituted to formula (28), integration gives

$$E_{\text{int}}^{n_c\text{b}-n_c\text{b}} = -Dn_c^2b^2\ln\frac{R}{P}. \tag{29}$$

Thus, the energy (26) of the system in its initial state is approximated by the sum of three terms. The two first terms strictly take into account the fine structure of the dislocation pile-ups (i.e. the specific distributions of dislocations within the pile-ups), while the third one is approximated by Eq. (29), which does not account for this fine structure. However, this approximation (when a pile-up is treated as a superdislocation) gives rather good results if the distance P (Fig. 4) is much larger than the pile-up length [26]. The latter must be smaller than $S/2$, and S is assumed to be always smaller (two or more times, see below) than P in the model. Therefore, the pile-up length must be four or more times smaller than P, and the approximation of superdislocations in calculating the term (29) is thus proved.

The energy of the GB dislocation ensemble in its final state (Fig. 4(b)) consists of the six terms

$$\tilde{W}_2 = 4E_{\text{self}}^{\Delta} + 4E_\tau^{\Delta} + 2E_\tau^{\text{pile-up}} + 2E_{\text{int}}^{\Delta_1-\Delta_2} + 2E_{\text{int}}^{\Delta_1-\Delta_3} + 2E_{\text{int}}^{\Delta_1-\Delta_4}, \tag{30}$$

where E_{self}^{Δ} denotes the self-energy of a disclination dipole, E_τ^{Δ} the work spent to transfer the GB dislocations resulted from the splitting under the shear stress τ, $E_\tau^{\text{pile-up}}$ the work spent to transfer all GB dislocations (from their initial positions) belonging to the pile-ups, under the shear stress τ, $E_{\text{int}}^{\Delta_i-\Delta_j}$ the energy of interaction between the ith and jth disclination dipoles ($i \neq j$, $i = 1,2,3$, $j = 2,3,4$).

Let us consider the self-energies of the disclination dipoles. In the framework of our model, the strength magnitude ω of the disclinations compos-

ing all the dipoles is the same, and the distance $(L-p)$ between two disclinations composing one dipole is the same for all the disclination dipoles. Therefore, each of the dipoles is characterized by the same energy [18]

$$E^{\Delta}_{\text{self}} = \frac{D\omega^2(L-p)^2}{2}\left(\ln\frac{R}{L-p} + \frac{1}{2}\right) + n_{\text{d}}\frac{Db_1^2}{2}, \quad (31)$$

where the second term on r.h.s. represents the sum core energy of all dislocations modeled through the disclination dipoles.

The shear stress τ acts on the climbing GB dislocations which compose the disclination dipoles. The work spent to climb n_{d} dislocations within one disclination dipole is

$$E^{\Delta}_{\tau} = -\tau b_1 \sin 2\phi\left(p + \frac{b_1}{\omega}\sum_{i=1}^{n_{\text{d}}}(i-1)\right) = \quad (32)$$

$$-\tau b_1 \sin 2\phi\left(p + \frac{b_1 n_{\text{d}}(n_{\text{d}}-1)}{2\omega}\right).$$

This work is the same for all the disclination dipoles under consideration (Fig. 4(b)).

The GB dislocations of each pile-up consequently move under the shear stress τ action from their initial positions $x = x_i$, to the new positions at the triple junctions ($x = 0$). The work spent to the transfer of all the GB dislocations of a pile-up is

$$E^{\text{pile-up}}_{\tau} = -\tau b\sum_{i=1}^{n_{\text{c}}}|x_i|. \quad (33)$$

Now let us consider the energy of interaction between the disclination dipoles. In doing so, first, for definiteness, we calculate the energy $E^{\Delta_1-\Delta_3}_{\text{int}}$ that characterizes interaction between the first and third disclination dipoles. The component $\sigma^{\Delta_1}_{xy}$ of the stress field of the first dipole in the coordinate system $Ox'y'$ (Fig. 4(b)) is as follows

$$\sigma^{\Delta_1}_{x'y'} = D\omega\left(\frac{(x'-x_{01})(y'-y_{01})}{(x'-x_{01})^2 + (y'-y_{01})^2}\right. \quad (34)$$

$$\left. -\frac{(x'-x_{02})(y'-y_{02})}{(x'-x_{02})^2 + (y'-y_{02})^2}\right),$$

where L denotes the length of the GB facet where the first dipole is located, $p = L-(1/\omega)(n_{\text{d}}-1)b_1$ is the interspacing between the positive disclination of the first dipole and the triple junction, $x_{01} = S\sin\phi$, $y_{01} = L+S\sin\phi$, $x_{02} = T-p\sin 2\phi$, $y_{02} = T'-p\cos 2\phi$, and $T = P\sin\phi$, $T' = P\cos 2\phi$. The energy of the interaction between the first disclination dipole and a dislocation being a structural element of the third dipole reads

$$E'^{\Delta_1-\Delta_3}_{\text{int}} = -b_1\int_{-R}^{0}\sigma^{\Delta_1}_{x'y'}(x',y')\,\mathrm{d}x', \quad (35)$$

with R being the screening length for stress fields of the disclination dipoles. The energy of the interaction between the disclination dipoles is given as

$$E^{\Delta_1-\Delta_3}_{\text{int}} = \frac{1}{l}\int_{y'_1}^{y'_2}E'^{\Delta_1-\Delta_3}_{\text{int}}(y')\,\mathrm{d}y', \quad (36)$$

where $y'_1 = p$, $y'_2 = L$ and $l = (b_1/\omega)$ is the distance between the neighboring GB dislocations being structural elements of a disclination dipole.

With Eq. (34) substituted to formula (35), integration in formulas (35) and (36) gives the interaction energy $E^{\Delta_1-\Delta_3}_{\text{int}}$ to be

$$E^{\Delta_1-\Delta_3}_{\text{int}} = E^{\Delta_2-\Delta_4}_{\text{int}} = \frac{D\omega^2}{4}\{\Psi_+(R,L,T,T',y',\phi)$$

$$-\Psi_+(R,p,T,T',y',\phi)-\Psi_+(0,L,T,T',y',\phi) \quad (37)$$

$$+\Psi_+(0,p,T,T',y',\phi)\}|^{y'_2}_{y'_1},$$

where

$$\Psi_{\pm}(s,l,t,t',y',\phi) = ((s+t)^2 + l^2 + (y'-t')^2$$

$$\pm 2l(y'-t')\cos 2\phi \mp 2l(s+t)\sin 2\phi)\ln((s+t)^2$$

$$+ l^2 + (y'-t')^2 \pm 2l(y'-t')\cos 2\phi \mp 2l(s$$

$$+ t)\sin 2\phi).$$

Geometry of the system composed of the second and fourth disclination dipoles is the same as with the system of the first and third dipoles. Therefore, the energy that characterizes pair interaction between the second and fourth disclination dipoles is also given by formula (37).

After some algebra similar to calculations of the energy $E^{\Delta_1-\Delta_3}_{\text{int}}$, we find formulas for other energies that characterize pair interactions between the disclination dipoles. These energies are as follows

$$E_{\rm int}^{\Delta_1-\Delta_2} = E_{\rm int}^{\Delta_3-\Delta_4} = \frac{D\omega^2}{4}\{\Psi_-(R,L,0,0,y',\phi) - \Psi_-(R,p,0,0,y',\phi) - \Psi_-(0,L,0,0,y',\phi) + \Psi_-(0,p,0,0,y',\phi)\}|_{y'_1}^{y'_2}, \quad (38)$$

$$E_{\rm int}^{\Delta_1-\Delta_4} = E_{\rm int}^{\Delta_2-\Delta_3} = \frac{D\omega^2}{4}\{\Psi_+(R,T',T,L,y',0) - \Psi_+(R,T',T,p,y',0) - \Psi_+(0,T',T,L,y',0) + \Psi_+(0,T',T,p,y',0)\}|_{y'_1}^{y'_2}. \quad (39)$$

Thus, we have calculated all terms figuring in the characteristic difference $\Delta\tilde{W} = \tilde{W}_2 - \tilde{W}_1$ between the energies of the final and initial states of the defect configuration (Fig. 4). If $\Delta\tilde{W}$ is negative (positive), the transformation of the defect configuration is energetically favorable (unfavorable, respectively). The dependence of $\Delta\tilde{W}$ on parameters of the system can be found from formulas (5), (22), (26), (29)–(33), (37)–(39). With these formulas, for $n_c = 5$, $L = 200b$, $P = 400b$, $R = 10^7 b$ and $\tau = 0.005G$, we have calculated the dependences of $\Delta\tilde{W}$ on disclination strength ω at different values of the angle ϕ that characterizes geometry of the triple junction (see Fig. 5). Following these dependences, the transformation is most favorable in the range of 2ϕ from 100 to 160°. Also, the magnitude of $\Delta\tilde{W}$ (that is, the energy gain due to the transformation when $\Delta\tilde{W} < 0$) decreases with an increase of the disclination strength ω (ranging from 0.05 to 0.1).

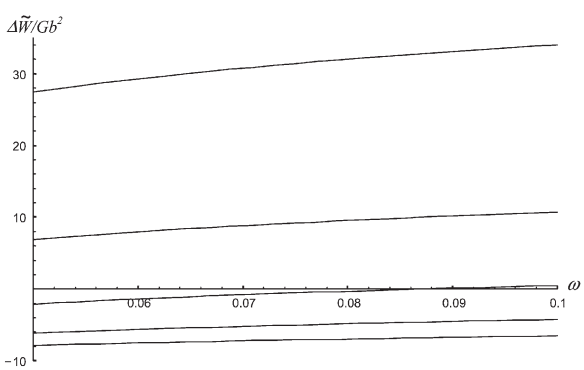

Fig. 5. Dependences of $\Delta\tilde{W}$ (in units of Gb^2) on disclination strength ω in the range of values of the triple junction angle 2ϕ = 60, 80, 100, 120 and 160° (from top to bottom).

4. Critical stress of crossover from grain boundary sliding to rotational deformation

The equation $\Delta\tilde{W} = \tilde{W}_2 - \tilde{W}_1 = 0$ allows one to calculate the critical shear stress τ_c at which the crossover from GB sliding to rotational deformation (Fig. 4) occurs. This equation may be written as follows

$$\tau_c = \frac{\tilde{W}'_2 - \tilde{W}_1(\tau_c)}{2b\sum_{i=1}^{n_c}|x_i(\tau_c)| + 4b_1 \sin 2\phi\left(p + \frac{b_1 n_d(n_d-1)}{2\omega}\right)}, \quad (40)$$

where $\tilde{W}'_2$ is given by formula (30) for $\tilde{W}_2$ with terms $4E_\tau^\Delta$ and $2E_\tau^{\text{pile-up}}$ removed.

In our numerical calculations of the critical shear stress τ_c given by formula (40), we will use the following characteristic values of parameters of nanocrystalline material and defect configuration under consideration. The Poisson ratio ν is equal to 0.3. Moduli of the GB dislocation Burgers vectors and disclination strength are taken as: b = 0.1 nm and $\omega = 0.1(\approx 5.7°)$. The number n_c is varied from 3 to 20 together with the distance L to keep the disclination strength ω constant. The distance p is also assumed to be constant and equal to l. These assumptions are considered reasonable based on the information available. As we will see later, actual form of the curves is not too sensitive on the values.

Now let us express the distance L through S and P, whose ratio $q = S/P < 1$. In doing so, we have

$$L = \frac{P(1-q)}{2\cos\phi}. \quad (41)$$

With formulas under discussion, for the above characteristic values of parameters, we have calculated the dependences of the critical shear stress τ_c on the grain size (diameter) P. These dependences are shown for $q = 0.5$ (Fig. 6(a)) and $q = 0.1$ (Fig. 6(b)), for different values of the triple junction angle 2ϕ. The curves τ_c (P) lie, in general, in different ranges of P because we have fixed ω. Therefore, increase in P leads to increase in both L and n_c, and this relation depends on the angle 2ϕ. For the sake of convenience, we attach the points cor-

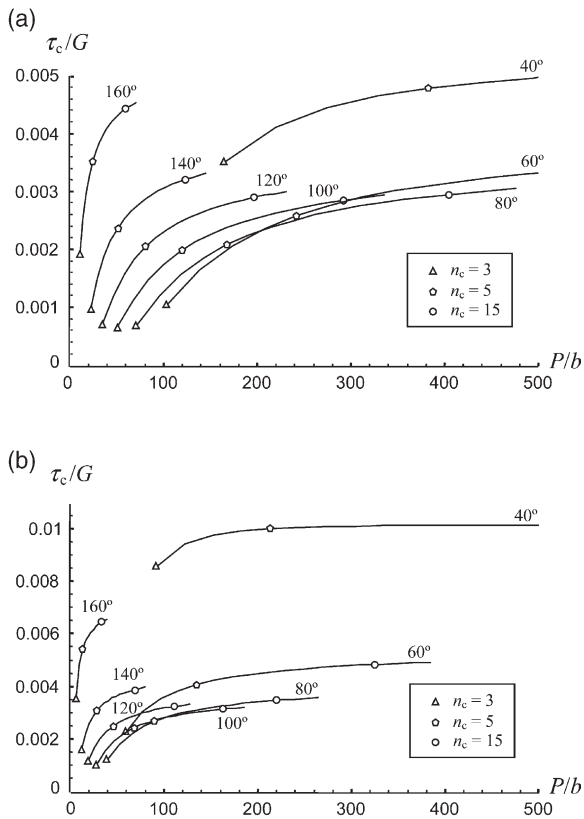

Fig. 6. Dependence of the critical stress τ_c on grain size P, (a) for $q = 0.5$ and (b) for $q = 0.1$, for different values of the triple junction angle 2ϕ given by figures at the curves. The numbers of GB dislocations n_c are shown by the triangles ($n_c = 3$), pentagons ($n_c = 5$) and circles ($n_c = 15$).

responding to $n_c = 3$ (triangles), 5 (pentagons) and 15 (circles) to every curve. The upper ends of the curves correspond to $n_c = 20$. As a result, we can additionally trace how τ_c depends on the angle 2ϕ when both the L and n_c keep constant.

From Fig. 6 it follows that τ_c decreases with the decrease of P (grain refinement). This is the main result of this section. It demonstrates that the smaller grains are rotated easier (they are rotated under the action of smaller critical stress τ_c) than the larger ones. Moreover, τ_c strongly depends on the grain shape (i.e. on q and 2ϕ). Increase in q leads to decrease in τ_c because larger q (for the fixed values of P and 2ϕ) needs smaller number n_c of GB dislocations to spread along the GB (or smaller dipole arm $L-p$). The dependence of τ_c on the angle 2ϕ is more complicated. For the fixed L and n_c, in the range of relatively small angles, $2\phi < 100°$, the critical stress τ_c decreases with increasing 2ϕ and achieves its minimum at $2\phi \approx 100°$. In the range of relatively large angles, $2\phi > 100°$, the critical stress τ_c increases with rising 2ϕ.

Thus, we can conclude that the smaller grains that are characterized by the larger q and $2\phi \approx 100°$, need the smaller critical stress τ_c to rotate.

5. Discussion and concluding remarks

In this paper, it has been theoretically revealed that the crossover from the GB sliding to the rotational mode of plastic flow in nanocrystalline materials can effectively occur via the splitting of gliding GB dislocations into climbing GB dislocations at triple junctions (Figs. 1, 2 and 4). The climbing GB dislocations form walls that move along GBs adjacent to the triple junction and cause crystal lattice rotation in the grain interior. Our theoretical analysis of the energy characteristics of the splitting has indicated that the splitting (Fig. 2) is energetically favorable in certain ranges of parameters of the system. More precisely, in contrast to the previously considered one in Ref. [7] situation with GB sliding which effectively occurs (changing its direction) at triple junctions with low values of the triple junction angle (2ϕ), the splitting (Fig. 2) effectively occurs at triple junctions with large values of the triple junction angle 2ϕ. That is, GB sliding and rotational mode act as alternative deformation mechanisms at triple junctions with different geometric parameters (ϕ). The experimentally detected [17,27–29] grain rotations in superplastically deformed nano- and microcrystalline materials where GB sliding is the dominant deformation mechanism, support the theoretical model developed here.

In general, superplasticity also involves the conventional lattice dislocation slip which is commonly viewed to provide accommodation for GB sliding [28,29] and supply lattice dislocations to GBs where the lattice dislocations split into GB dislocations being carriers of GB sliding [29]. In the context of our model describing the combined

action of the GB sliding and the rotational mode, we think that the lattice dislocations absorbed by GBs also enhance a climb of GB dislocations resulted from the splitting of gliding GB dislocations at triple junctions (Fig. 7). Actually, lattice dislocations absorbed by GBs commonly split into GB dislocations of the two types: gliding and climbing GB dislocations; see Fig. 7(a) and (b) where only the climbing dislocations are shown for simplicity. The climbing dislocations absorbed by one GB have the sum Burgers vector close to 0, because of a random character of absorption of lattice dislocations by GBs (Fig. 7(b)). At the same time, the mechanical stress causes a directional climb of GB dislocations, in which case after some time interval the dislocations with opposite Burgers vectors move towards each other, annihilate or form dipole configurations (Fig. 7(b)). The climbing GB dislocations resulted from the splitting of gliding dislocations at a triple junction break the balance between the Burgers vectors of GB dislocations generated due to absorption of lattice dislocations (Fig. 7(c)). The new dislocations that resulted from the splitting of gliding GB dislocations attract the corresponding dislocations resulted from the splitting of absorbed lattice dislocations and, then, they annihilate (Fig. 7(d)). In these circumstances, "an effective enhanced climb" of the Burgers vector is realized along the boundary due to annihilation of climbing GB dislocations, occurring simultaneously along the boundary (Fig. 7(d)).

The enhanced GB dislocation climb stimulated by conventional dislocation slip causes the two following effects crucially important for superplasticity in nanocrystalline materials: (i) plastic defor-

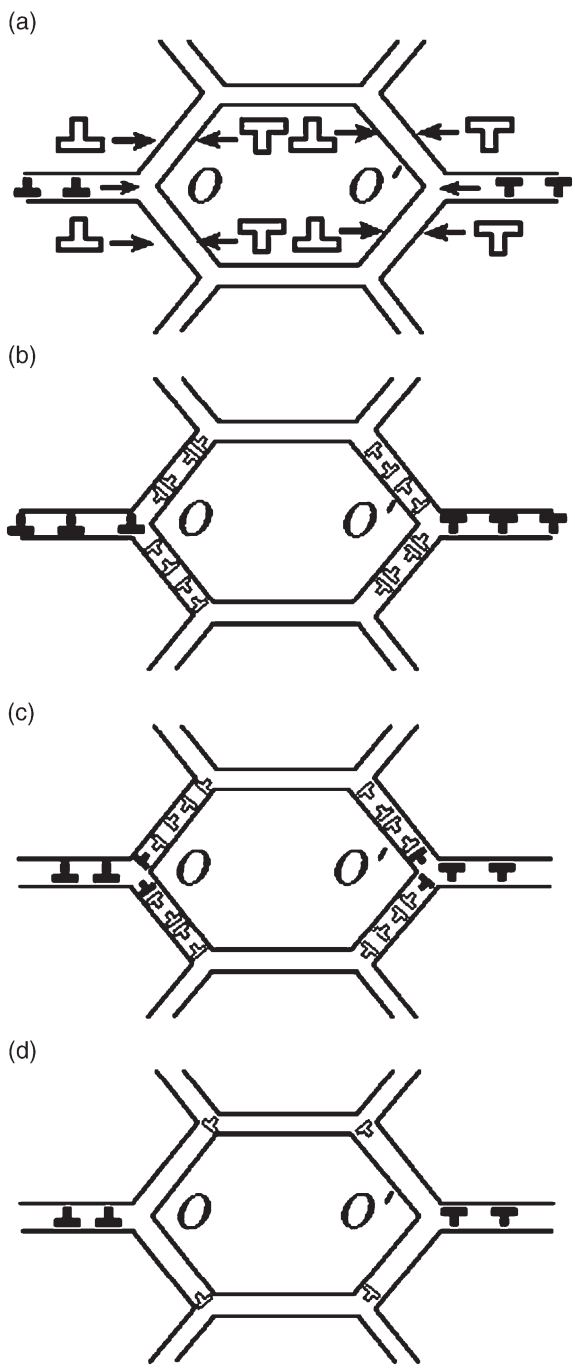

Fig. 7. Enhancement of climb of GB dislocations due to absorption of lattice dislocations by GBs. (a) Lattice dislocations (large open dislocation signs) and gliding boundary dislocations (small full dislocation signs) move under the shear stress action. (b) Climbing dislocations (small open dislocation signs) resulted from splitting of absorbed lattice dislocations form dipole configurations at GBs. (c) Head GB dislocations of pile-up split into climbing dislocations (full dislocation signs) at triple junctions O and O'. (d) Annihilation of climbing dislocations forming dipole configurations results in the formation of isolated climbing dislocations highly distant from triple junctions O and O'.

mation is spread in the direction perpendicular to the direction of the maximum shear stress action; (ii) triple junctions with large abutting angles, that do not conduct GB sliding [7], effectively conduct the crossover from the GB sliding to the rotational mode and, therefore, do not serve as stress concentrators enhancing the nucleation of microcracks. As a result of the effects (i) and (ii), neither plastic flow localization nor failure processes occur in a nanocrystalline material which, therefore, is capable of sustaining large plastic deformations.

The suggested representations on the combined action of GB sliding and rotational mode enhanced by conventional dislocation slip are indirectly supported by the experimentally detected [23] suppression of high-strain-rate superplasticity in heat-treated nanocrystalline materials. Actually, heat treatment results in annihilation of the GB dislocations generated due to conventional dislocation slip in nanocrystalline materials prepared by severe plastic deformation. Therefore, enhanced climb of GB dislocations from triple junctions does not occur causing suppression of the crossover from the GB sliding to the rotational mode. As a result, a nanocrystalline specimen after heat treatment does not exhibit high-strain-rate superplasticity.

Acknowledgements

This work was supported, in part, by the Office of US Naval Research (grant N00014-01-1-1020), the Russian Fund of Basic Research (grant 01-02-16853), Russian State Research Program on Solid-State Nanostructures, RAS Program “Structural Mechanics of Materials and Constructions”, St Petersburg Scientific Center, and “Integration” Program (grant B0026).

References

[1] Mohamed FA, Li Y. Mater Sci Eng A 2001;298:1.
[2] Padmanabhan KA. Mater Sci Eng A 2001;304–306:200.
[3] Koch CC, Morris DG, Lu K, Inoue A. MRS Bull 1999;24:54.
[4] Hahn H, Mondal P, Padmanabhan KA. Nanostruct Mater 1997;9:603.
[5] Hahn H, Padmanabhan KA. Philos Mag B 1997;76:559.
[6] Konstantinidis DA, Aifantis EC. Nanostruct Mater 1998;10:1111.
[7] Fedorov AA, Gutkin MYu, Ovid’ko IA. Acta mater 2003;51:887.
[8] Masumura RA, Hazzledine PM, Pande CS. Acta mater 1998;46:4527.
[9] Kim HS, Estrin Y, Bush MB. Acta mater 2000;48:493.
[10] Yamakov V, Wolf D, Phillpot SR, Gleiter H. Acta mater 2002;50:61.
[11] Fedorov AA, Gutkin MYu, Ovid’ko IA. Scr Mater 2002;47:51.
[12] Gutkin MYu, Ovid’ko IA, Pande CS. Rev Adv Mater Sci 2001;2:80.
[13] Murayama M, Howe JM, Hidaka H, Takaki S. Science 2002;295:2433.
[14] Ovid’ko IA. Science 2002;295:2386.
[15] Gutkin MYu, Kolesnikova AL, Ovid’ko IA, Skiba NV. J Metast Nanocryst Mater 2002;12:47.
[16] Gutkin MYu, Kolesnikova AL, Ovid’ko IA, Skiba NV. Philos Mag Lett 2002;81:651.
[17] Mukherjee AK. Mater Sci Eng A 2002;322:1.
[18] Romanov AE, Vladimirov VI. In: Nabarro FRN, editor. Dislocations in solids, vol. 9. Amsterdam: North Holland; 1992. p. 191–402.
[19] Seefeldt M. Rev Adv Mater Sci 2001;2:44.
[20] Gutkin MYu, Mikaelyan KN, Romanov AE, Klimanek P. Phys Status Solidi (a) 2002;193:35.
[21] McFadden SX, Misra RS, Valiev RZ, Zhilyaev AP, Mukherjee AK. Nature 1999;398:684.
[22] Mishra RS, Valiev RZ, McFadden SX, Islamgaliev RK, Mukherjee AK. Philos Mag A 2001;81:37.
[23] Islamgaliev RK, Valiev RZ, Misra RS, Mukherjee AK. Mater Sci Eng A 2001;304–306:206.
[24] Mura T. In: Herman H, editor. Advances in material research, vol. 3. New York: Interscience; 1968. p. 1–108.
[25] Eshelby JD, Frank FC, Nabarro FRN. Philos Mag 1951;42:351.
[26] Hirth JP, Lothe J. Theory of dislocations. New York: Wiley, 1982.
[27] Valiev RZ, Langdon TG. Acta Metall 1993;41:949.
[28] Zelin MG, Mukherjee AK. Mater Sci Eng A 1996;208:210.
[29] Valiev RZ, Alexandrov IV. Nanostructured materials prepared by severe plastic deformation. Moscow: Logos, 2000 [in Russian].